

Impregnation of S-layer protein isolated from extremophilic *Bacillus licheniformis* NARW 02 onto titanium phosphate ceramic enhances uranium removal from aqueous solution

R. Selvakumar^{1,*}, S. Aravindh¹,
J. Ravichandran², U. Kamachi Mudali³,
C. Anandbabu⁴ and Baldev Raj⁵

¹Nanobiotechnology Laboratory, Nanotech Research Facility, PSG Institute of Advanced Studies, Peelamedu, Coimbatore 641 004, India

²Department of Chemistry, PSG College of Technology, Peelamedu, Coimbatore 641 004, India

³Corrosion Science and Technology Group, Corrosion Science and Technology Division, Indira Gandhi Centre for Atomic Research, Kalpakkam 603 102, India

⁴Department of Biotechnology, PSG College of Technology, Peelamedu, Coimbatore 641 004, India

⁵PSG Institutions, Peelamedu, Coimbatore 641 004, India

In the present study, bioceramic was prepared by impregnating surface layer protein (S-layer) isolated from extremophilic bacteria *Bacillus licheniformis* NARW 02 onto sol-gel-derived titanium phosphate (TiP) ceramic. The prepared bioceramic was used for adsorption of uranium ions from aqueous solution and compared with control lacking S-layer protein. The distribution coefficient value of TiP and bioceramic for uranium adsorption was 100.65 and 432.48 ml/g respectively. This study indicates that the bacterial S-layer can be potentially used to enhance the adsorption efficiency of the ceramics used in separation of uranium from waste water.

Keywords: *Bacillus licheniformis*, extremophilic bacteria, titanium phosphate ceramic, uranium.

THE direct interaction between microbes and contaminants through biosorption strongly determines the fate of the contaminant in the environment¹. Biosorption is mainly achieved through various ionizable groups like carboxylate and phosphate groups present in the lipopolysaccharides, teichoic acid and peptidoglycan layers of microbial cell wall. Other than these groups, microbial capsules and S-layer proteins (crystalline arrays of glycoprotein subunits located at the outermost part of the cell wall) are also involved in such sorption process². These S-layers proteins vary from one species to the other and have their own selectivity and reactivity towards various ionic groups like uranium³.

Similar to microorganisms, inorganic ion exchangers have been reported to possess good binding capacity towards nuclear waste⁴. Recently, microporous metal

phosphates have garnered attention for such applications. Surfactant-based preparation of mesoporous titanium phosphate has been reported to sequester 99% of long-lived radionuclides like Pu(IV) in aqueous solution through ion-exchange process⁵. Lebedev *et al.*⁶ reported that titanium phosphate has greater ability to bind to cesium present in the liquid radioactive waste when compared to zirconium phosphate. Amorphous spherically granulated titanium phosphate showed efficient uranium removal⁷. These studies clearly indicate that titanium phosphate has higher binding capacity towards radioactive waste and can be used as an ideal candidate for removal of radionuclides. Recently, many scientists have tried to couple the biological system with inorganic adsorbents to prepare a bioceramic. The main advantage of these bioceramic is the possibility of exploring the properties of biological structures after the biocomponent is supported through a ceramic matrix⁸.

In this study we have isolated an extremophilic, uranium and radiation-resistant S-layer containing bacteria, *Bacillus licheniformis* NARW 02 from uranium ore. The S-layer from these bacteria was separated and used to prepare a bioceramic for removal of uranium from aqueous solution.

Uranium ore was collected from Uranium Corporation of India Limited (UCIL), Tumallapalle mines, Andhra Pradesh and UCIL-Narwapahar mines, Jharkhand, India. Microorganisms were isolated from these samples using modified enriched nutrient agar medium (g/l) – beef extract (3); yeast extract (2); NaCl (5); peptone (5); agar (15); enriched filtrate (1000 ml; filtrate prepared by mixing 1 g of the mine soil in 100 ml of distilled water followed by filtration in Whatman No. 1 filter paper).

Uranium tolerance studies were carried out according to Prakash *et al.*⁹. Nutrient broth amended with various concentrations of uranyl nitrate (0, 250, 500, 700, 1000 mg/l) was inoculated with 0.5% v/v (~2 × 10⁸ cfu/ml) of selected bacterial cultures and incubated at 37°C in a shaker at 120 rpm. Optical density of the culture suspension was recorded every 12 h at 600 nm using UV-Vis spectrophotometer (T90, UK). The organisms having higher tolerance towards uranium were selected for further studies. The biosorption of uranium onto the bacterial cell wall before and after exposure was deduced using high-resolution transmission electron microscopy (HR-TEM). The most resistant bacteria were further subjected to gamma radiation studies. Nutrient-free mid log phase bacteria washed with 100 mM potassium phosphate buffer (pH 7.0) were exposed to 2.5, 5.0, 7.5 and 10.0 kGy gamma radiation from a ⁶⁰Co source in a Gamma Radiation Chamber (GC 5000, BRIT, India)¹⁰. Irradiated cultures were serially diluted and viability was checked. *Deinococcus radiodurans* ATCC 13939 and *Escherichia coli* MTCC 1687 were used as positive and negative control respectively. The most resistant isolates were identified using 16S rRNA partial sequencing.

*For correspondence. (e-mail: selvabiotech@gmail.com)

Bacterial S-layer was extracted according to Sleytr *et al.*¹¹. In brief, 24 h grown bacterial cells were harvested from culture broth and washed with 50 mM *Tris* HCl buffer (pH 7.2). The washed cells were re-suspended in 5M guanidine HCl and incubated for 2 h at 20°C. The content was centrifuged at 40,000 g for 30 min at 4°C and the supernatant was dialysed against 10 mM CaCl₂ for 12 h at 4°C. The dialysate was centrifuged at 40,000 g for 30 min at 4°C. Pellets were re-suspended in 10 mM CaCl₂ and stored at 4°C till further use. The S-layer protein was quantified using Lowry's methods. Titanium phosphate (TiP) ceramic was prepared using sol-gel process according to Onoda and Yamaguchi¹². Bioceramic was prepared according to Göbel *et al.*¹³. In brief, 1:1 ratio of S-layer protein and TiP was mixed for impregnation using *N*-(3-dimethyl-aminopropyl)-*N'*-ethylcarbodi-imide hydrochloride (EDC) dissolved in 50 mM *Tris* HCl buffer (pH 7.2). The content was incubated overnight, centrifuged and the pellet stored at -20° C until further use. The S-layer, ceramic and bioceramic were analysed using HR-TEM at 80 kV on carbon-coated copper grid followed by energy dispersive spectrometry (EDX) and selected area electron diffraction (SAED) studies. The attachment of S-layer onto the ceramic was visualized using epi-fluorescence microscopy (Nikon Eclipse E600) after staining with 10 µl of fluorescein sodium salt¹⁴. Image-Pro Plus 6.3 software was used for image analysis.

The protein adsorption/desorption onto/from the ceramic was tested by column studies. A phosphate buffered saline (PBS; pH 7.5) equilibrated column containing bioceramic was prepared under room temperature. The flow-through fractions of PBS from column were analysed for protein using Lowry's method every 2 h. Desorption of adsorbed proteins was accomplished by applying 1% SDS in PBS buffer (pH 7.5) to the column and desorption fractions were analysed. The total binding capacities (TBCs) were calculated using the following formula

$$\text{TBC \%} = \frac{(\text{Initial protein conc.} - \text{Final protein conc.})}{(\text{Initial conc.})} \times 100. \quad (1)$$

Batch-mode studies were carried out by agitating 100 mg of ceramic and bioceramic in 10 ml of uranium (U) solution of desired concentration at 150 rpm at room temperature (initial pH 4.5 adjusted using 1N HCl). The content was placed in a rotary shaker at 130 rpm for 24 h. After a known incubation period, the biocer materials were separated by centrifugation at 3000 rpm for 5 min and the residual level of uranium present in the solution was estimated using Arsenazo III method¹⁵. Langmuir isotherm was employed to study the adsorption efficiency. For column studies, bioceramic at desired quantity was suspended in fresh PBS (pH 7.5) and deposited on top of the filter membrane (sintered porous polypropylene filter membrane (~10–20 µM) with 5 mm thickness and 47 mm diameter) to have a bed volume of 5 mm. The flow rate,

adsorbent dosage, volume and concentration of uranium used were varied from 1 to 3 ml/min, 0.5 to 1.5 g, 10 to 30 ml and 50 to 100 mg/l respectively. Silicon tubing was used for the connections.

K_d was calculated to elucidate the adsorption capacity of adsorbent towards uranium. K_d (ml/g) was calculated according to eq. (1)

$$K_d = ((C_0 - C_e)/C_e) \times (V/M), \quad (2)$$

where C_0 and C_e are amount of uranium sorbed and remaining in the solution (mg/l) respectively, V the volume of the liquid phase (ml) and M is the mass of the solid phase (g).

Thirty-nine bacteria were isolated from the uranium ore samples collected from Tumallapalle and Narwapahar mines. All the isolates were subjected to initial uranium concentration of 750 mg/l in nutrient broth and screened for uranium tolerance. Only five isolates could resist 750 mg/l of uranium. LD50 value was calculated by subjecting the isolates to varying concentrations of uranium. Among the five isolates, NARW 02 and NARW 11 showed maximum tolerance to uranium up to 979 and 982 mg/l respectively. Such tolerance to higher uranium concentration may be attributed to mobilization (protonation, chelation and chemical transformation)/immobilization (precipitation, crystallization, sorption, uptake and intracellular sequestration) processes¹⁶ that influence the balance of metal species between soluble and insoluble phases. The HR-TEM analysis after exposure to uranium clearly showed uranium precipitation (Figure 1). This bioprecipitation of uranium onto the cell wall may be facilitated by the involvement of deprotonated phosphate and carboxyl moieties on the cell wall¹⁷. The exposure of NARW 02 and NARW 11 to higher concentration of uranium led to the swelling of cells and deflagellation (Figure 1c and d). As the concentration of uranium was increased from 250 to 1000 mg/l, the cell viability of NARW 02 and NARW 11 was in the range 4.03–3.85 × 10⁶ and 4.1–3.88 × 10⁶ cfu/ml respectively. Such viability of the cell may be due to the sequestration of uranium into its oxide form as reported by Choudhary and Sar¹⁷ with *Pseudomonas aeruginosa*.

Further, all the five isolates were subjected to various gamma radiation dosages (0, 2.5, 5, 7.5 and 10 kGy) and their viability was checked. *D. radioduran* ATCC 13939 and *E. coli* MTCC 1687 were taken as positive and negative control respectively. As the dosage of gamma radiation was increased from 0 to 7.5 kGy, the viability of the cell decreased (Table 1). After 7.5 kGy of radiation exposure, NARW 02 and NARW 11 showed 5 ± 1.4 × 10³ and 5 ± 5.7 × 10³ cfu/ml viability respectively. This was 3.3-fold higher when compared to the well-reported radiation-resistant bacteria *D. radioduran* ATCC 13939 (Table 1). On further increase of dosage from 7.5 to 10 kGy, all the bacterial strains lost their viability. Such tolerance to

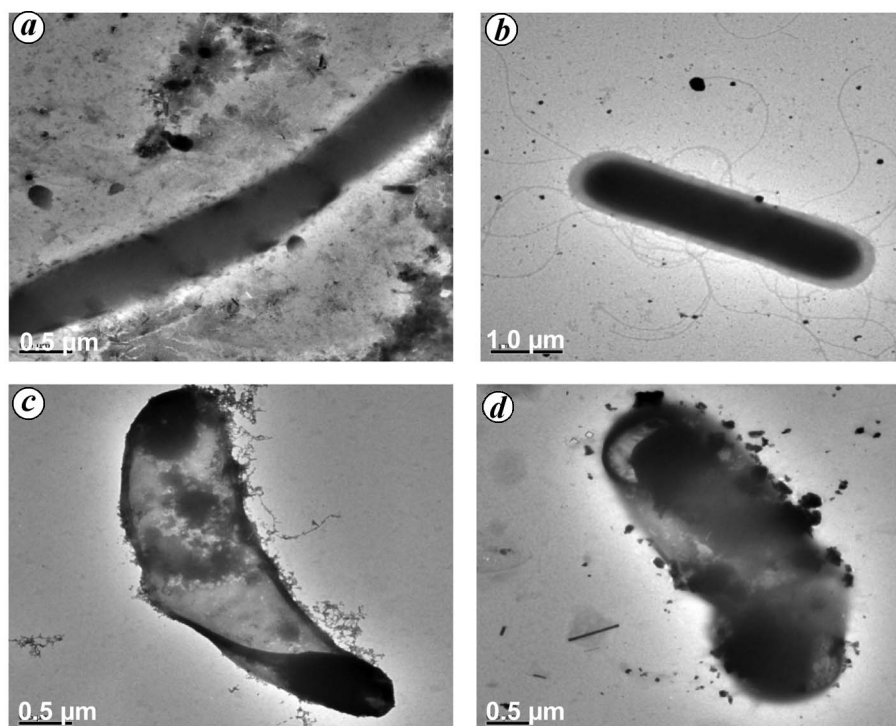


Figure 1. HR-TEM analysis of cells before (*a, b*) and after (*c, d*) uranium exposure. (*a, c*, NARW 02 bacteria; *b, d*, NARW 11 bacteria).

Table 1. Cell viability after gamma radiation exposure

Heterotrophic bacterial isolates	Gamma radiation/bacterial enumeration (cfu/ml)			
	0 kGy	2.5 kGy	5 kGy	7.5 kGy
TMPL 02	$16.5 \pm 0.7 \times 10^5$	$15.5 \pm 0.7 \times 10^5$	$6 \pm 1.4 \times 10^3$	$1.15 \pm 0.2 \times 10^3$
TMPL 10	$11 \pm 1.4 \times 10^5$	$3.5 \pm 2.1 \times 10^5$	$1.6 \pm 0.6 \times 10^4$	$1.5 \pm 0.7 \times 10^3$
NARW 07	$13.5 \pm 0.7 \times 10^5$	$10.5 \pm 0.7 \times 10^4$	$6 \pm 1.4 \times 10^3$	$1.1 \pm 0.1 \times 10^3$
NARW 02	$14.5 \pm 0.7 \times 10^5$	$4 \pm 1.4 \times 10^5$	$4 \pm 1.4 \times 10^4$	$5 \pm 1.4 \times 10^3$
NARW 11	$18 \pm 1.4 \times 10^5$	$11 \pm 1.4 \times 10^5$	$6.5 \pm 0.7 \times 10^4$	$5 \pm 5.7 \times 10^3$
Control				
<i>Escherichia coli</i>	$1.25 \pm 0.4 \times 10^5$	0	0	0
<i>Deinococcus radiodurans</i>	$1.75 \pm 0.4 \times 10^5$	$6 \pm 1.4 \times 10^5$	$2.5 \pm 0.7 \times 10^4$	$1.5 \pm 0.7 \times 10^3$

TMPL, Tumallapalle mine ore; NARW, Narwapahar mine ore. Mean value of triplicate \pm standard deviation.

gamma radiation may be due to strong DNA repair mechanism¹⁸, the regulatory proteins¹⁹ or S-layer²⁰. NARW 02 and NARW 11 isolates were identified as *B. licheniformis* and *B. anthracis* respectively (NCBI GenBank accession nos JX469598.1 and JX469599.1 respectively) based on 16S ribosomal RNA sequencing. Considering the pathogenic reports of *B. anthracis*, further studies were carried out only using *B. licheniformis* NARW 02.

Bioceramic was prepared by impregnating extracted S-layer protein from *B. licheniformis* NARW 02 onto the TiP ceramic. The characterization studies clearly indicated the impregnation of S-layer onto the ceramic. The UV-Vis spectroscopy showed an absorbance peak between 260 and 280 nm wavelength, indicating the pre-

sence of proteinaceous compound in the solution. The control TiP ceramic material did not show any absorbance peak for proteins. The TBC of the S-layer protein onto the ceramic was found to be 715 $\mu\text{g/ml}$ in 1 g of TiP. The S-layer proteins and bioceramic material after staining with fluorescein, emitted green fluorescence; however such fluorescence was not present in control TiP (Figure 2). The FTIR spectroscopy also showed shift in peak indicating the adsorption of S-layers onto the ceramics (Figure 3). The 1636 cm^{-1} band corresponding to C=O shifted to lower frequency of 1627 cm^{-1} with a decrease in absorbance. The 1465 cm^{-1} band shifted to a higher frequency of 1469 cm^{-1} . There was appreciable shift of 1022 cm^{-1} band to 1072 cm^{-1} , indicating the involvement of phosphate group in the S-layer impregnation process.

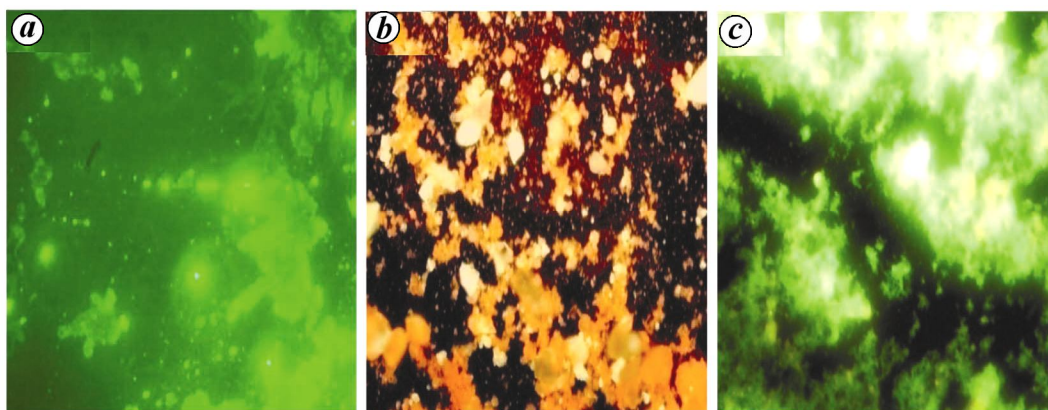


Figure 2. Epifluorescence microscopic images of S-layer, titanium phosphate (TiP) and bioceramic. *a*, S-layer from *Bacillus licheniformis*; *b*, TiP; *c*, *B. licheniformis* S-layer-coated TiP bioceramic.

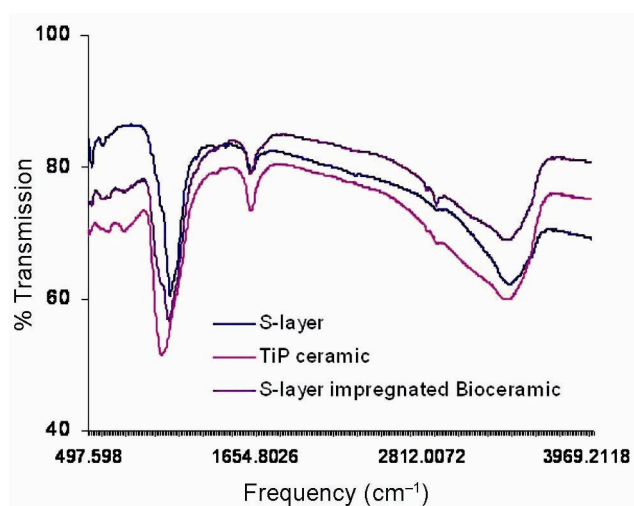


Figure 3. FTIR spectroscopy of S-layer, TiP and bioceramic.

The 1546 cm^{-1} band found in S-layer corresponding to the combination of NH band with C–N peptide of the protein was found to be absent. The isolated S-layer, structure, shape and size of TiP ceramic and S-layer-impregnated ceramic were studied using HR-TEM (Figure 4). The isolated S-layer was highly porous and appeared like a mesh (Figure 4*a*). The TiP particles were below 30 nm and irregular in shape (Figure 4*b*). When S-layer was impregnated onto the TiP ceramic, a thin layer of S-layer protein was observed on the surface of the ceramic indicating the formation of bioceramic (Figure 4*c*). The SAED pattern of TiP showed its crystalline nature. However, on impregnation of S-layer onto the ceramic, the crystallinity of TiP was found to decrease indicating the binding of S-layer protein to the ceramic (Figure 4*b* and *c* insets respectively). EDX spectroscopy clearly showed the presence of titanium and phosphate in TiP ceramic (Figure 5).

During the initial adsorption studies, TiP ceramic and bioceramic were compared for their adsorption efficiency

towards uranium in batch mode. The S-layer impregnated bioceramic showed maximum uranium removal of 84.43%, whereas control could remove only 53.88% with 100 mg/l of uranium. Hence impregnation of S-layer from *B. licheniformis* strain onto TiP increased the adsorption of uranium by 30.55%. Based on this result further experiments were carried out only with S-layer-impregnated TiP bioceramic. The uranium uptake by bioceramic was found to increase with contact time and remained constant after equilibrium (90 min; Figure 6). The percentage removal increased from 57.67 to 84 on increasing the contact time from 10 to 360 min. However, as the concentration of uranium was increased from 25 to 1000 mg/l, the percentage removal decreased from 89.24 to 6.99 (Figure 7). The initial rapid phase of adsorption may be due to increased number of vacant sites available for adsorption at the initial stages; as a result, there exists an increased concentration gradient between adsorbate in solution and adsorbate in adsorbent²¹. The K_d value of TiP and bioceramic for uranium adsorption was 100.65 and 432.48 ml/g respectively. The removal data were fitted onto Langmuir isotherm represented by the following equation²²

$$C_e/q_e = 1/Q_0b + C_e/Q_0, \quad (3)$$

where C_e is the concentration of uranium solution (mg/l) at equilibrium, the constant Q_0 signifies the adsorption capacity (mg/g) and b is related to the energy of adsorption (l/mg). The linearity of the plots (R^2) indicates that uranium adsorption follows Langmuir isotherm model. The values of Q_0 and b were calculated from the slope and intercept of the Langmuir plot and compared with the other adsorbents in the literature (Table 2). The uranium adsorption capacity (mg/g) and energy of adsorption (b) for bioceramic were found to be 59.96 mg/g and 0.336 l/mg respectively. Our bioceramic was found to be superior to many reported adsorbents^{23–26} (Table 2). The effect of the bioceramic on uranium adsorption was also

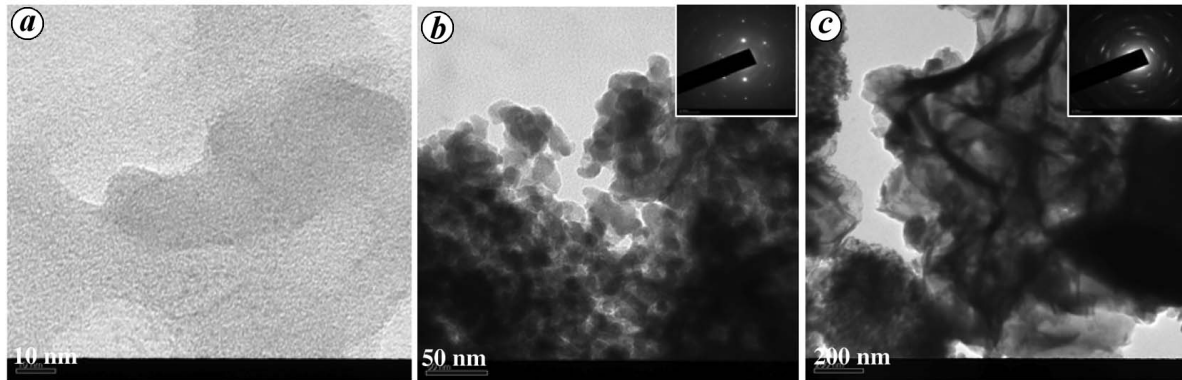


Figure 4. HR-TEM images of S-layer, TiP and bioceramic. *a*, S-layer isolated from *B. licheniformis* NARW 02; *b*, TiP ceramics. (Inset) SAED pattern; *c*, S-layer impregnated bioceramics. (Inset) SAED pattern.

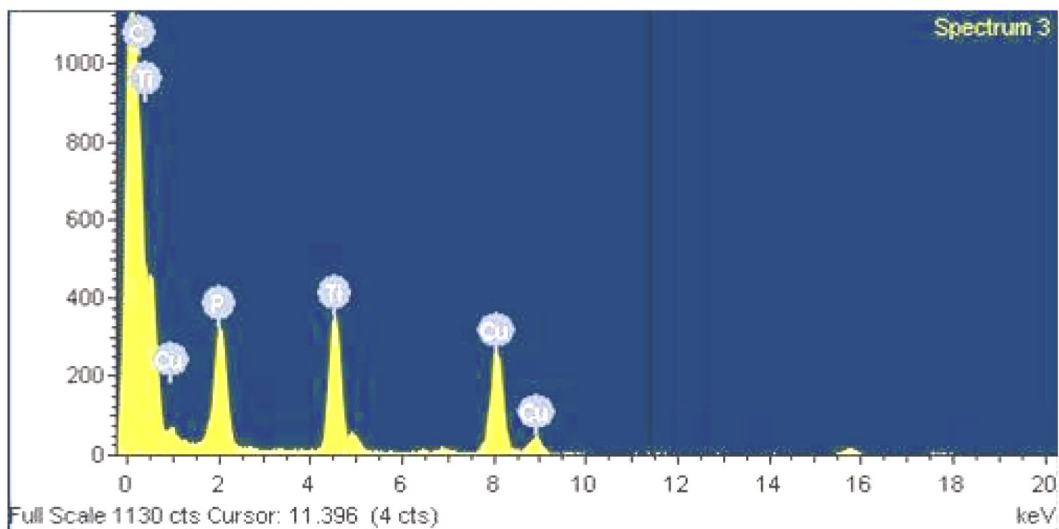


Figure 5. EDX spectroscopy of TiP.

Table 2. Comparison of uranium adsorption with the existing literature

Adsorbent	Q_0 (mg g ⁻¹)	Reference
Bi-functionalized biocomposite adsorbent	50.25	23
Hematite	3.5	24
Nanoporous silica PEI	12.2	25
Manganese oxide coated zeolite	15.1	26
S-layer impregnated titanium phosphate	59.96	Present study

deduced using microfiltration column studies. The column-mode studies were carried out by varying flow rate, adsorbent dosage, volume and concentration of uranium. The increase in flow rate from 1 to 3 ml/min decreased the removal of adsorbates from 93.53% to 87.44%. Whereas when adsorbent dosage was increased from 0.5 to 1.5 g, the percentage removal increased from 92.16 to 96.76 (Table 3). These results show that the number of available sites for uranium adsorption increase with increase in adsorbent dosage. When the volume of inflow

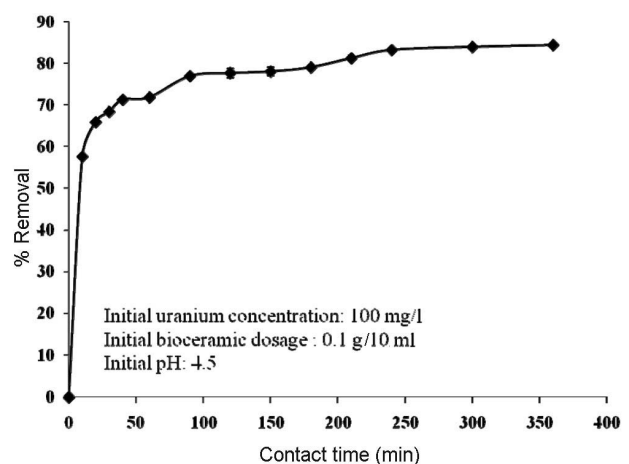


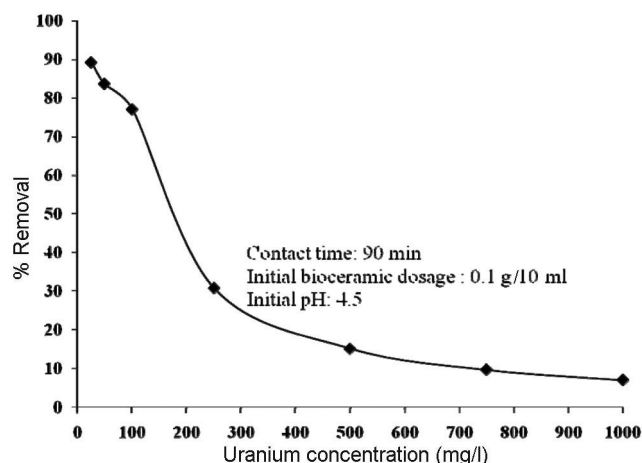
Figure 6. Effect of contact time on uranium removal.

was increased from 10 to 30 ml/min, the adsorption of uranium decreased slightly from 93.04% to 89.07% (Table 3). Similarly, when the uranium concentration was

Table 3. Effect of various parameters on uranium adsorption in column studies using bioceramic

Flow rate (ml/min) ^a	Uranium adsorption (%)	Adsorbent dosage (g) ^b	Uranium adsorption (%)	Adsorbate conc. (mg/l) ^c	Uranium adsorption (%)	Volume (ml/min) ^d	Uranium adsorption (%)
1	93.53 ± 0.69	0.5	92.16 ± 1.49	100	91.67 ± 0.60	10	93.04 ± 1.39
2	90.42 ± 0.74	1.0	93.48 ± 0.77	75	94.94 ± 0.49	20	91.21 ± 1.19
3	87.44 ± 0.60	1.5	96.76 ± 0.94	50	96.61 ± 0.77	30	89.07 ± 1.66

^aBioceramic: 1 g; volume 10 ml; uranium conc: 100 mg/l. ^bFlow rate: 1 ml/min; volume 10 ml; uranium conc: 100 mg/l. ^cFlow rate: 1 ml/min; volume 10 ml; bioceramic: 1 g. ^dFlow rate: 1 ml/min; bioceramic: 1 g; uranium conc: 100 mg/l. Mean value of triplicate ± standard deviation.

**Figure 7.** Effect of concentration on uranium removal.

decreased from 100 to 50 mg/l, the percentage removal increased from 91.66 to 96.61 (Table 3). These results are in correlation with earlier studies^{23–26}.

The bioceramic made of bacterial S-layer and TiP showed increased uranium removal when compared to control TiP. The K_d value for uranium adsorption was found to increase from 100.65 to 432.48 ml/g after impregnation of S-layer onto TiP ceramics. The batch and column-mode studies indicated that the bioceramic was efficient in removal of uranium from aqueous solution when compared to control TiP and hence can be used as efficient adsorbent for the removal of uranium from waste waters of radioactive industry.

- Selenska-Pobell, S., Diversity and activity of bacteria in uranium waste piles. In *Interactions of Microorganisms with Radionuclides* (eds Keith-Roach, M. and Livens, F.), Elsevier Sciences, Oxford, UK, 2002, pp. 225–253.
- Sleytr, U. B., I. Basic and applied S-layer research: an overview. *FEMS Microbiol. Rev.*, 1997, **20**, 5–12.
- Merroun, M. L., Nedelkova, M., Heilig, M., Rossberg, A., Hennih, C. and Selenska-Pobell, S., Interaction of uranium with bacterial strains, isolated from extreme habitats: EXAFS studies. FZR-Report. 2005, 419, p. 37.
- Choppin, G. R. and Khankhasayev, M. K., Chemical separation technologies and related methods of nuclear waste management: applications, problems, and research needs. In NATO Science Series, Klumer Academic Publishers, Dordrecht, The Netherlands, 1998, vol. 53, p. 11.

- Li, X. S., Courtney, A. R., Yantasee, W., Mattigod, S. V. and Glen Fryxell, E., Templated synthesis of mesoporous titanium phosphates for the sequestration of radionuclides. *Inorg. Chem. Commun.*, 2006, **9**, 293–295.
- Lebedev, V. N., Mel'nik, N. A. and Rudenko, A. V., Sorption of cesium on titanium and zirconium phosphates. *Radiochemistry*, 2003, **45**, 149.
- Zakutevskyy, O. I., Psareva, T. S. and Strelko, V. V., Sorption of U(VI) ions on sol-gel-synthesized amorphous spherically granulated titanium phosphates. *Russ. J. Appl. Chem.*, 2012, **85**, 1366–1370.
- Botcher, H., Soltmann, U., Mertig, M. and Pompe, W. G., Biocers: ceramics within incorporated microorganisms for biocatalytic, biosorptive and functional materials development. *J. Mater. Chem.*, 2004, **14**, 2176–2188.
- Prakash, O. *et al.*, *Geobacter daltonii* sp. an Fe(III)- and uranium(VI)-reducing bacterium isolated from a shallow subsurface exposed to mixed heavy metal and hydrocarbon contamination. *Int. J. Syst. Evol. Microbiol.*, 2010, **60**, 546–553.
- Yuan, M. *et al.*, *Deinococcus gobiensis* sp., an extremely radiation-resistant bacterium. *Int. J. Syst. Evol. Microbiol.*, 2009, **59**, 1513–1517.
- Sleytr, U. B., Huber, C., Ilk, N., Pum, D., Schuster, B. and Egelseer, E. M., S-layers as a tool kit for nanobiotechnological applications. *FEMS Microbiol. Lett.*, 2007, **267**, 131–144.
- Onoda, H. and Yamaguchi, T., Synthesis of titanium phosphates with additives and their powder properties for cosmetics. *Mater. Sci. Appl.*, 2012, **3**, 18–23.
- Göbel, C., Schuster, B., Baurecht, D., Sleytr, U. B. and Pum, D., S-layer templated bioinspired synthesis of silica. *Colloids Surf. B*, 2010, **75**, 565–572.
- Pital, A., Janowitz, S. L., Hudak, C. E. and Lewis, E. E., Direct fluorescent labeling of microorganisms as a possible life-detection technique. *Appl. Microbiol.*, 1966, **14**, 119–123.
- Khan, M. H. and Evans, W. P. N., Spectrophotometric determination of uranium with arsenazo-III in perchloric acid. *Chemosphere*, 2006, **63**(7), 1165–1169.
- Haferburg, G., Reinicke, M., Merten, D., Büchel, G. and Kothe, E., Microbes adapted to acid mine drainage as source for strains active in retention of aluminum or uranium. *J. Geochem. Explor.*, 2007, **92**, 196–204.
- Choudhary, S. and Sar, P., Uranium biomineralization by a metal resistant *Pseudomonas aeruginosa* strain isolated from contaminated mine waste. *J. Hazard. Mater.*, 2011, **186**, 336–343.
- Kira, S. *et al.*, Genome of the extremely radiation-resistant bacterium *Deinococcus radiodurans* viewed from the perspective of comparative genomics. *Microbiol. Mol. Biol. Rev.*, 2001, **65**(1), 44–79.
- Gupta, A. K. *et al.*, Proteomic analysis of global changes in protein expression during exposure of gamma radiation in *Bacillus* sp. HKG 112 isolated from saline soil. *J. Microbiol. Biotechnol.*, 2011, **21**(6), 574–581.
- Kotiranta, A. K., Ito, H., Haapasalo, M. P. and Lounatma, K., A radiation sensitivity of *Bacillus cereus* with and without a

crystalline surface protein layer. *FEMS Microbiol. Lett.*, 1999, **179**, 275–280.

21. Selvakumar, R. *et al.*, As(V) removal using carbonized yeast cells containing silver nanoparticles. *Water Res.*, 2011, **45**, 583–592
22. Langmuir, I., The adsorption of gases on plane surfaces of glass, mica and platinum. *J. Am. Chem. Soc.*, 1918, **40**, 1361.
23. Aytas, S., Alkim Turkozu, D. and Gok, C., Biosorption of uranium (VI) by bi-functionalized low cost biocomposite adsorbent. *Desalination*, 2011, **280**, 354–362.
24. Shuibo, X., Chun, Z., Xinghuo, Z., Jing, Y., Xiaojian, Z. and Jingsong, W., Removal of uranium (VI) from aqueous solution by adsorption of hematite. *J. Environ. Radioact.*, 2009, **100**, 162.
25. Jung, Y., Kim, S., Park, S. J. and Kim, J. M., Application of polymer-modified nanoporous silica to adsorbents of uranyl ions. *Colloids Surf. A*, 2008, **33**, 162.
26. Han, R., Zou, W., Wang, Y. and Zhu, L., Removal of uranium(VI) from aqueous solutions by manganese oxide coated zeolite: discussion of adsorption isotherms and pH effect. *J. Environ. Radioact.*, 2007, **93**, 127.

ACKNOWLEDGEMENTS. We thank the Indira Gandhi Centre for Atomic Research (IGCAR), Kalpakkam for providing financial support. We also thank Dr Rani P. George, Corrosion Science and Technology Division; Dr B. Venkataraman, Dr Balasundhar, Radiological Safety and Environment Group, IGCAR; Dr T. Subba Rao, Water and Stream Chemistry Division, BARC Facilities, Kalpakkam; Uranium Corporation of India and PSG Management, Coimbatore for help rendered throughout the study.

Received 2 December 2013; revised accepted 1 May 2014

Geochemistry of pegmatites from South Delhi Fold Belt: a case study from Rajgarh, Ajmer district, Rajasthan

Kumar Batuk Joshi¹, Soumya Ray¹, Deepak Joshi¹ and Talat Ahmad^{1,2,*}

¹Department of Geology, University of Delhi, Delhi 110 007, India

²University of Kashmir, Srinagar 190 006, India

On the basis of geochemical studies, pegmatites emplaced in the Rajgarh Group of Delhi Supergroup in the South Delhi Fold Belt have been classified into three groups. They show a variety of rare earth element enrichment patterns, LREE/HREE values and Eu anomalies. The geochemical affinities of these pegmatites suggest their calc-alkaline nature, volcanic arc granite signature in tectonic discrimination diagrams (Nb vs Y and Rb vs Nb + Y) and a probable S-type parentage as inferred from their high A/CNK value,

peraluminous character, presence of high normative corundum and abundance of garnet and muscovite. These features have been related to subduction-related processes which might have generated the parent granitic melt forming these pegmatites.

Keywords: Geochemical studies, granitic melt, pegmatites, subduction.

THAT pegmatites result from magmatic differentiation of granitic systems^{1–7} is almost unanimously agreed upon by geologists and therefore referred to as ‘granitic pegmatites’, although pegmatitic textures can result in igneous rocks of all compositions⁸. Pegmatites are representative of late-stage residual fraction of silicic melt that accumulate in the granitic parent magma itself or intrude the surrounding rocks⁹. However, it is not always mandatory for the pegmatites to be in close spatial association with the parent granite^{6,10}. The volatile-rich, residual, pegmatitic melt seems to favour stability at lower temperatures at large distances from the parent plutonic source^{6,11}. The enrichment of rare elements (Be, Ta, Li, Sn, Bi, W, Mo, Cu) and volatiles in the late residual magma^{6,12} renders the granite, pegmatites and hydrothermal veins subsequently formed substantially mineralized, economically viable and sought after. However, it is to be borne in mind that these rare element enriched-granitic pegmatites constitute about less than 1% by volume of the pegmatite terrain they are a part of¹³ and that not all pegmatite bodies can be exploited for their mineral content. One of the most rudimentary principles underlying geochemistry is the enrichment of the compatible and incompatible elements in the fractionating minerals and residual melt respectively. These preferential behaviours and consequent chemical signatures have formed the basis of characterization and differentiation of one rock from the other and even give an account of their possible evolution and parentage. The accentuated trace element signatures that pegmatite inherit from their granitic sources can be used to fingerprint their origin¹³.

The NE–SW trending Aravalli–Delhi orogen which runs across Rajasthan separates the Marwar and Mewar cratons and comprises of the Aravalli Fold Belt and the Delhi Fold Belt¹⁴. The South (SDFB) and North Delhi Fold Belts form the principal divisions of the Proterozoic Delhi Fold Belt^{15–17} and expose rocks of the Delhi Supergroup¹⁴. The SDFB comprises of the western Sendra basin (consisting of the Barotiya and Sendra Group of rocks) and the eastern Bhim basin (consisting of the Rajgarh and Bhim Group of rocks)¹⁸ which are separated by an inlier of pre-Delhi rocks^{14,19}. Several hypotheses regarding the evolution of the Delhi Fold Belt have been put forward by previous workers. Heron²⁰ proposed that sedimentation took place in intracontinental fault-bound grabens. However, the more popular diachronous development model was proposed by Sinha-Roy^{15,16}, wherein

*For correspondence. (e-mail: tahmad001@yahoo.co.in)